

1 Article

2 Hydrophilic and Hydrophobic Mesoporous Silica 3 Derived from Rice Husk Ash as a Potential Drug 4 Carrier

5 Supakij Suttiruengwong^{1*} Sommai Pivsa-Art and² Metta Chareonpanich²

6 ¹ Department of Materials Science and Engineering, Faculty of Engineering and Industrial Technology,
7 Silpakorn University, Sanamchandra Palace Campus, Nakhon Pathom, 73000, Thailand;

8 suttiruengwong_s@su.ac.th

9 ² Department of Material and Metallurgical Engineering, Faculty of Engineering, Rajamangala University of
10 Technology Thanyaburi, Pathumthani 12110, Thailand; sommai.p@en.rmutt.ac.th

11 ³ Department of Chemical Engineering, Faculty of Engineering, Kasetsart University,
12 Bangkok, 10900 Thailand; fengmtc@ku.ac.th

13 * Correspondence: suttiruengwong_s@su.ac.th; Tel.: +66-34-241-708

14

15 **Abstract:** This work describes the preparation of mesoporous silica by the green reaction of rice
16 husk ash (RHA) with glycerol, followed by the modification and the potential use as a drug carrier.
17 The reaction was carried out at 215 °C for 2 h. The solution was further hydrolyzed with deionized
18 water and aged for various times (24, 48, 120, 360, 528 and 672 h) before calcinations at 500 °C for 24
19 h. Further treatment of prepared mesoporous silica was performed using trimethylmethoxysilane
20 (TMMS) to obtain hydrophobic Mesoporous silica. For all synthesized silicas, silica contents were
21 as high as 95%wt, whereas organic residues were less than 3%wt. RHA-glycerol showed the highest
22 specific surface area with smallest pore diameter (205.70 m²/g, 7.46 nm) when aged for 48 h. The
23 optimal hydrolysis-ageing period of 120 h resulted in 500.7 m²/g BET surface area, 0.655 cm³/g pore
24 volume and 5.23 nm pore diameter. The surface modification of RHA-glycerol was succeeded
25 through the reaction with TMMS as confirmed by FTIR. Ibuprofen was selected as a model drug for
26 the adsorption experiments. The adsorption under supercritical CO₂ was carried out at isothermal
27 temperature of 40 °C and 100 bar, % ibuprofen loading of TMMS modified mesoporous silica
28 (TMMS-g-MS) was 6 times less than mesoporous silica aged for 24 h (MS-24h) due to the
29 hydrophobic nature of modified mesoporous silica, not surface and pore characteristics. The release
30 kinetics of ibuprofen-loaded mesoporous silicas were also investigated *in vitro*. The release rate of
31 ibuprofen-loaded MS-24h was much faster than that of ibuprofen-loaded TMMS-g-MS, but
32 comparable to the crystalline ibuprofen. The slower release rate was attributed to the diffusion
33 control and the stability of hydrophobic nature of modified silica. This would allow the design for
34 the controlled release drug delivery system.

35 **Keywords:** mesoporous silica; surface area; rice husk ash; hydrolysis-ageing time, hydrophobicity

36

37 1. Introduction

38 Mesoporous silica materials have many superior advantages in which they can be employed in
39 a wide range of industries such as catalysts, absorbents, nano-carrier for drug, pharmaceuticals,
40 insulation materials, rubbers, electronics, reinforced composite in plastics, cosmetics and biomedical
41 and dental materials. Thailand, as a rice-growing and rice export country, around 30 million tonnes
42 of rice in Thailand are produced during 2015-16 [1]. Rice husks are often burnt for an energy recovery
43 and consequently produced rice husk ash (RHA). RHA obtained in general rice mill consists of more
44 than 80% silica and high contents of char residues and small traces. It possesses a low specific surface

45 area and pore sizes. The recovery of purer amorphous and reactive silica from RHA can be obtained
46 through low temperature calcinations and chemical treatments [2], hence obtaining the silicas with
47 lesser impurities and specific physicochemical properties i.e. tunable specific surface area and pore
48 sizes, which can be beneficial and value-added in some niche products. Many methods [3] are readily
49 employed for the preparation of the mesoporous silica from RHA, including pre- and post-chemical
50 treatments [4-6], calcination, the use of templating agent [7-9], and sol-gel method [9]. Chemicals used
51 in sol-gel, ageing time, drying method and calcination conditions are all important factors affecting
52 the pore structures and specific surface area. Especially, the ageing of gel is one of the key steps to
53 ensure the maturity of the gel network, which the condensation reaction is completed.

54 The environmentally-benign depolymerization reaction of silicate network and RHA in
55 existence of glycerol near 200 °C was reported [10]. Reactive gels retained the mesoporous nature
56 after hydrolysis and calcination [10]. In addition, the reactive gels can be further modified chemically
57 e.g. hydrophobic gels, or alternatively used to synthesize other porous materials [11] and aerogels.
58 The reaction of RHA with other bifunctional alcohols to produce reactive gels has also been studied
59 [12]. In this work, it was aimed to employ the use of green solvent and renewable resources to prepare
60 mesoporous silica. The effect of hydrolysis-ageing periods on the physic-chemical properties was
61 investigated. The surface treatment of silica is also carried out. Ibuprofen is selected as a model drug.
62 The drug adsorption in supercritical carbon dioxide on hydrophilic and hydrophobic mesoporous
63 silica was performed to determine the adsorption capability. Finally, the release kinetics are
64 measured and evaluated.

65 2. Materials and Methods

66 2.1. Materials

67 Rice husks (RH) were supplied by rice mill, Nakhon Pathom province, Thailand. Glycerol 99.9%
68 was purchased from Sigma-Aldrich Laborchemikalien, Germany. Ibuprofen ((RS)-2-(4-
69 isobutylphenyl) propionic acid) ≥99% was purchased from Fluka, China. Aerosil 200 fumed silica was
70 kindly supplied by Evonik, Thailand.

71 2.2. Preparation of mesoporous silica from rice husks

72 The procedure for preparing mesoporous silicas from rich husks (RH) was presented elsewhere
73 [10, 12]. Briefly, RH was calcined at 500 °C for 24 h to obtain RHA starting materials. RHA and
74 glycerol (1:10 w/v) were mixed at 200±1 °C, 2 h. The excess glycerol was evacuated after the reaction.
75 The excess deionized water was added for hydrolysis and the mixture was aged at room temperature
76 for various times (24, 48, 120, 360, 528 and 672 h; referred as hydrolysis-ageing periods). Aged gels
77 were washed with distilled water several times and dried at 105°C, 24 h. Dried gels were again
78 calcined at 500°C for 24 h (a product referred to MS-00h; 00 is hydrolysis-ageing period). The
79 experiment was repeated for hydrolysis-ageing time of 24 h using Aerosil A2000 (FS) for comparison.

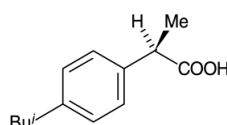
80 2.3. Surface modification of mesoporous silica

81 The surface modification of MS-24h was performed in a mixture of water/ethanol (25/75 by
82 volume). 0.3 g of Trimethoxymethylsilane (TMMS) and 1 g of MS was introduced into 100 ml of
83 solution mixture at 60 °C, 8 h. The product was filtered and washed several times finally dried at
84 60°C, 8 h. The product named TMMS-m-MS was kept in desiccator for further analysis.

85 2.4. Drug adsorption

86 To study the potential use of mesoporous silica, ibuprofen (>99% puris, mw=206.3 g/mol, Sigma
87 Aldrich) was selected as a model drug. The chemical structure of ibuprofen is representen in Figure
88 1. Ibuprofen (RS)-2-(4-isobutylphenyl)propionic acid (C₁₃H₁₈O₂) is is another non-steroidal anti-

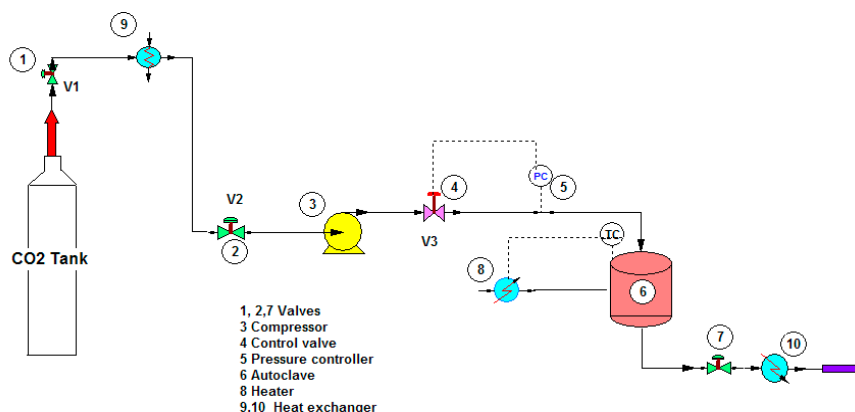
89 inflammatory drug (NSAIDs) and has been reported by many works for drug adsorption under
 90 supercritical carbon dioxide due to its good dissolution. For the drug loading or adsorption
 91 experiments, 0.05-0.1 g of as-synthesized mesoporous silica (MS and TMMS-m-MS) were weighted
 92 into the filter paper and placed inside the autoclave chamber as represented in Figure 2. The
 93 experiment setup was described by Suttiruengwong S. [13]. Briefly, after closing the autoclave, the
 94 preheat carbon dioxide at the temperature of 40 ± 1 °C was fed into the autoclave, where the inside
 95 temperature was also 40 ± 1 °C. After that, CO₂ was slowly fed into the autoclave until the desired
 96 pressure (50, 60, 80, 90 and 100 bar) was reached. It should be noted that the critical temperature and
 97 pressure of carbon dioxide was 31°C and 73.7 bar respectively. The samples were left shaking in the
 98 autoclave for 48 hours to ensure the equilibrium. CO₂ gas mixture was then vented out at the constant
 99 flowrate. The samples were then weighted again to determine the percent loading or adsorption. The
 100 drug loading could be calculated from the increase in weight of the samples. The increase in weight
 101 of the samples indicates the adsorption of drugs in the samples. Alternatively, the concentration of
 102 drugs in the samples can be determined by UV-vis spectroscopy ($\lambda_{\text{max}} = 221$ nm) using Beer Lambert's
 103 law. The amount of CO₂ in the autoclave at the equilibrium was calculated from the known volume
 104 and CO₂ density. The values of CO₂ density were taken from NIST standard reference database [14].



105

106

Figure 1. Chemical structure of ibuprofen.



107

108

Figure 2. Schematic representation of drug loading experiment under supercritical carbon dioxide.

109

2.5. *In vitro* release experiments

110

111

112

113

114

115

116

117

118

The accumulative release of ibuprofen was determined using a simulate gastric fluid, 0.1 M HCl (pH 1.2) according to pharmacopoeias (i.e. DAB, USP, Eu. Ph.). The sample (drug crystals or loaded mesoporous silica powder) was weighed and placed in the basket together with a filter paper to prevent the loss of the sample powder during the transferring of the basket to the dissolution medium as shown in Figure 3. The amount of the drug was selected so that the sink condition was ensured. The basket was then fixed under the agitator and immersed into the vessel containing 900 ml of dissolution medium (0.1 M HCl) at constant temperature of 37 ± 0.1 °C. The stirring speed was kept at 100 min^{-1} . The 2 mL aliquots were withdrawn at predetermined time intervals, filtered through a 0.45 μm Nylon filter and analyzed using UV-VIS spectrophotometer (PI Instrument, UK).

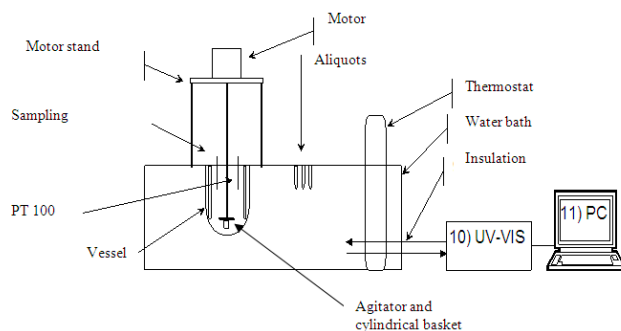


Figure 3. Dissolution experiment assembly.

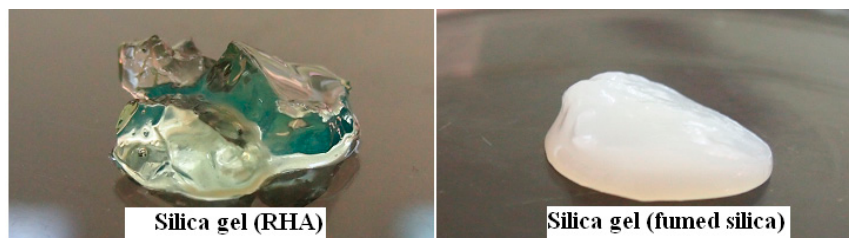
119

120

121 3. Results

122 3.1. Physico-chemical properties of as-synthesized mesoporous silica

123 Fumed silica was used to ensure the reaction of glycerol for comparison. Starting with two
 124 different silica sources, fumed silica and RHA, the reaction of glycerol with fumed silica was more
 125 favorable than RHA probably due to much higher surface area and high purity of fumed silica. After
 126 hydrolysis, the immediately formed gel derived from fumed silica indicated the faster condensation
 127 reaction between silanol groups of colloidal silica particles whereas the gel derived from RHA was
 128 set after few hours. Figure 4 showed the transparent silica gel prepared from RHA compared to
 129 opaque gel prepared from fumed silica.



130

Figure 4. Digital images of gels from RHA (left) and fumed silica (FS) (right) as starting silica sources.

131

132 Table 1 displays the silica compositions and textural characteristics of starting silica materials
 133 (RHA), synthesized mesoporous silica (MS) with various hydrolysis-ageing times, commercial fumed
 134 silica (FS) and mesoporous silica obtained from FS (FS-1). The pore characteristics however changed
 135 as the ageing time increased to about 48 h. The longer ageing time did not change specific surface
 136 area, pore diameter and volume significantly. The maturity of the gels reached at 120 h as the
 137 condensation became very slow. The BET surface area of MS also increased substantially compared
 138 to RHA whereas in the case of fumed silica the BET surface area almost unaffected by this method.
 139 However, for pore volumes of MS and FS-1 increased. The pore diameter was reduced for MS, but
 140 increased in case of FS-1. The N₂ isotherm of MS-24h and FS-1 showed type IV isotherm with H3
 141 hysteresis, suggesting mesoporous characteristics containing slit-shaped pores.

142

143

144

145

146

147

148

149

150

151

152 **Table 1.** Textural characteristics of starting silica, mesoporous silica materials, surface-modified silica materials
 153 and fumed silica

Samples	$I_{\text{Si-OH}}/I_{\text{Si-O-Si}}$ ratio	Compositions (%)					Weight loss ^b	Surface area BET (m ² /g)	Pore volume (cm ³ /g)	Pore diameter (nm)
		SiO ₂ ^a	K ₂ O ^a	CaO ^a	MnO ^a	Fe ₂ O ₃ ^a				
RHA	-	86.74	7.53	2.19	0.23	0.27	3.02	46.26	0.315	27.41
MS-24h	3.628	94.5	0.2	0.3	0.1	0.1	4.84	149.4	0.549	14.69
MS-48h	2.286	95.1	0.2	0.3	0.1	-	4.28	205.7	0.384	7.46
MS-120h	2.070	95.0	0.1	0.2	0.1	-	4.49	500.7	0.655	5.23
MS-360h	1.700	95.5	0.2	0.2	0.1	-	4.06	453.8	0.518	4.56
MS-672h	1.241	95.3	0.2	0.2	0.1	-	4.19	451.9	0.613	6.42
TMMS-m-MS	-							144.3	0.544	14.83
FS**		≥99.8 ^c	-	-	-	-	-	200±25 ^c	0.338	8.96
FS-1		98.9 ^b	-	-	-	-	1.05 ^b	208	0.820	24.56

154 ^aXRF results with subtraction of weight loss from TGA analysis, ^bTGA analysis, ^cmaterials data sheet

155

156

157

158

159

160

161

162

163

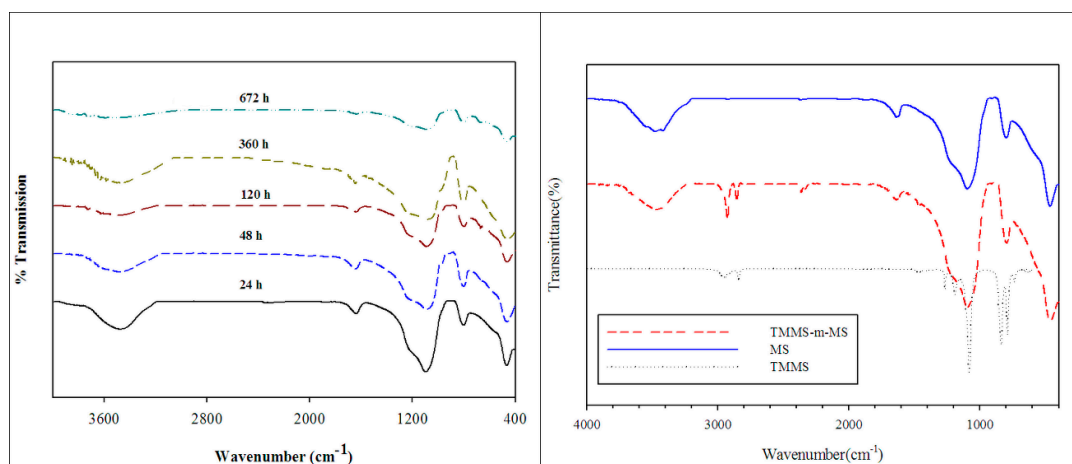
164

165

166

167

FTIR spectra (Figure 5 (a)) of the samples hydrolyzed and aged for various time periods indicated the characteristic peak of silica similar to other works [2, 13, 15]. The characteristic peak of silanol groups and adsorption of water showed at 3000-3400 cm⁻¹. The peak at 950 cm⁻¹ was assigned to Si-OH deformation. The asymmetry stretching of Si-O-Si occurred at 1000-1200 cm⁻¹. The existence of surface hydroxyl groups could be estimated by normalizing the intensity of Si-OH ($I_{\text{Si-OH}}$) at 950 cm⁻¹ with the intensity of Si-O-Si ($I_{\text{Si-O-Si}}$) at 1100 cm⁻¹ as shown in Table 1. A decrease in this ratio indicated the decrease in surface hydroxyl groups. As expected, the samples after calcinations at 500 °C for 24 h had hydrophilic characteristics with existence of silanol groups. The longer hydrolysis-ageing time gave rise to the tendency to reduce silanol groups. FTIR spectra of the surface modification of MS with TMMS as demonstrated in Figure 5(b) revealed the existing of Si-CH₃ at 2860 cm⁻¹ [16]. The reduction of hydroxyl group intensities around 3300-3500 cm⁻¹ also implied that some modification took place. The sample was also observed by the floatation on the water.

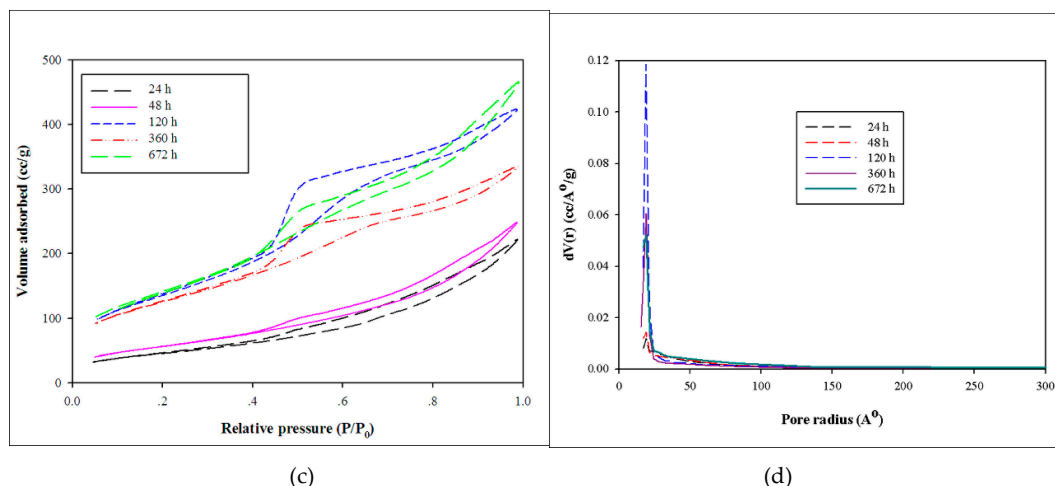


168

169

(a)

(b)

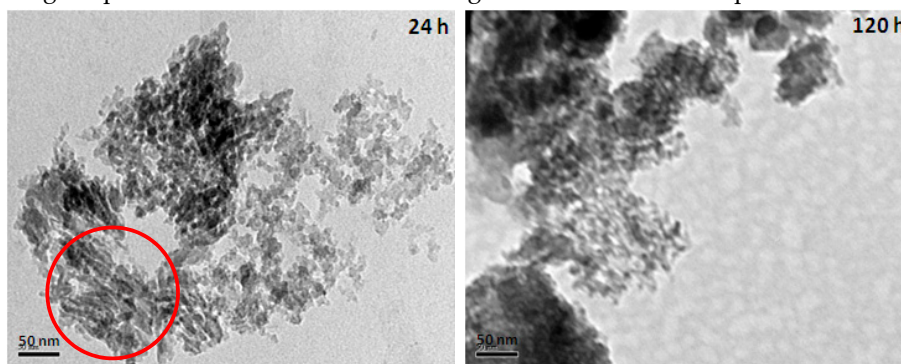


170
171

172 **Figure 5.** FTIR spectra of mesoporous silica prepared by various hydrolysis-ageing time periods (a), surface-
173 modified silica (TMMS-m-MS) (b) and (c) N₂ sorption isotherms of mesoporous silica and (d) PSD curves for
174 various hydrolysis-ageing periods.

175 The N₂ sorption isotherms of mesoporous silicas (Figure 5 (c)) were affected by different
176 hydrolysis-ageing periods. The hydrolysis-ageing periods was less than 48 h, isotherms consisted of
177 a steep uprising step at the P/P₀= 0.1, followed by greater increasing step from P/P₀ of 0.45 whereas
178 the PSD and pore diameter of all samples were insignificantly changed. The shapes of N₂ sorption
179 isotherms were considered to be type IV with H3 hysteresis loop for samples with less than 120 h of
180 hydrolysis-ageing periods. At above 120 h of hydrolysis-ageing periods, isotherms exhibited type IV
181 with H3 and H2 hysteresis loop, indicating more complex pores with different sizes and shapes [17].
182 The gel started to form after hydrolysis and at the beginning hour, the condensation reaction was
183 reversible and experienced the backward hydrolysis reaction until optimal time of 120 h was reached.
184 The BET surface area and pore volumes of samples tended to increase whereas an average pore size
185 decreased in the first 48 h.

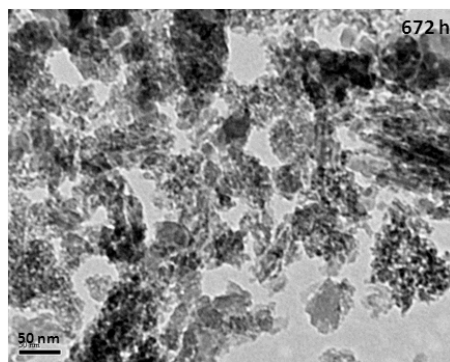
186 The TEM images of mesoporous silicas with various hydrolysis-ageing periods were showed in
187 Figure 6. Silica particles at short hydrolysis-ageing period (24 h) exhibited pores with slit shapes (red
188 circles) whereas, at 120 h of hydrolysis-ageing periods and longer, smaller and denser pores with
189 some existing slit pores were observed. This finding was confirmed the sorption isotherms analysis.



190
191

(a) ..

(b)



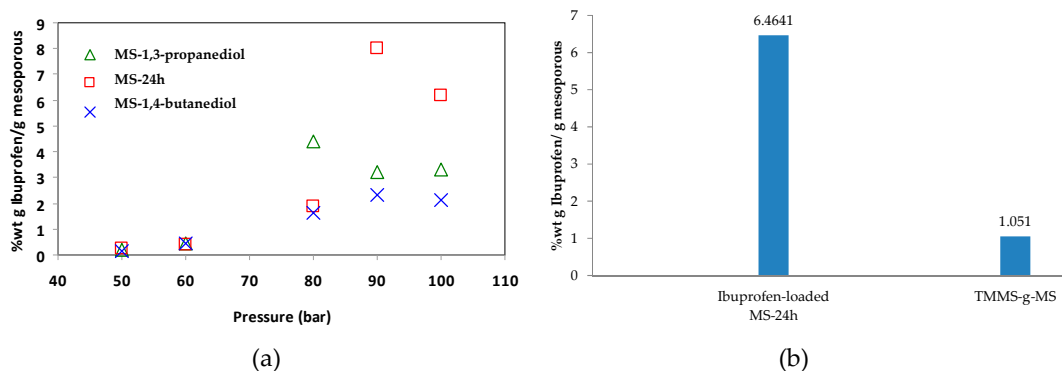
(c)

192

193

194 **Figure 6.** TEM images of mesoporous silica at the hydrolysis-aging periods of 24 h (a), 120 h (b) and 672 h (c).195 **3.2. Drug loading**

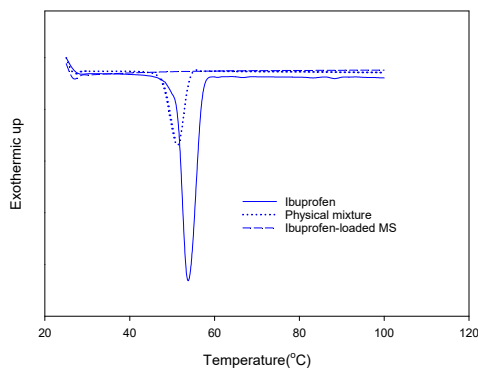
196 The adsorption of ibuprofen under different mesoporous silica derived from glycerol, 1,3-
 197 propanediol and 1,4-butanediol was investigated. The synthesized mesoporous silica using 1,3-
 198 propanediol and 1,4 butanediol was described elsewhere [12]. The reaction with diols led to more
 199 hydrophobic nature as explained by S. Suttiruengwong [12]. From Figure 7(a), under supercritical
 200 carbon dioxide conditions (above 80 bar), the adsorption of ibuprofen was more than 2 folds and was
 201 independent of MS types. It should be also noted that these mesoporous silicas had different specific
 202 surface area, pore size and pore volume. MS-24 could take up very high ibuprofen loading, especially
 203 at 90 and 100 bar. Therefore, the pressure of 100 bar was chosen for loading MS-24 and TMMS-g-MS.
 204 The samples; MS and TMMS-g-MS, were chosen for comparison in order to ensure the effect of the
 205 surface modification alone as both samples had fairly similar specific surface area, pore volume and
 206 diameter as illustrated in Table 1. DSC thermograms were recorded for the samples shown in Figure
 207 8. It was observed that the melting peak disappeared for Ibuprofen loaded MS sample whereas the
 208 typical ibuprofen crystalline and physical mix (ibuprofen and MS mixture) showed the melting peak
 209 at 53 °C and 50 °C respectively. This was evident that the state of ibuprofen after adsorption was
 210 amorphous.



211

212

213 **Figure 7.** Concentration of (a) ibuprofen loaded mesoporous silicas with different pressure at 40 °C and (b)
 214 ibuprofen loaded MS-24 and TMMS-g-MS at 90 bar, 40 °C where equilibrium concentration of Ibuprofen in
 215 CO₂ was 0.0740 %wt.



216

217

Figure 8. DSC thermograms of crystalline ibuprofen, physical mixture (MS and ibuprofen) and ibuprofen-loaded MS.

218

219

3.3. Release kinetics of ibuprofen-loaded mesoporous silicas

220

221

222

223

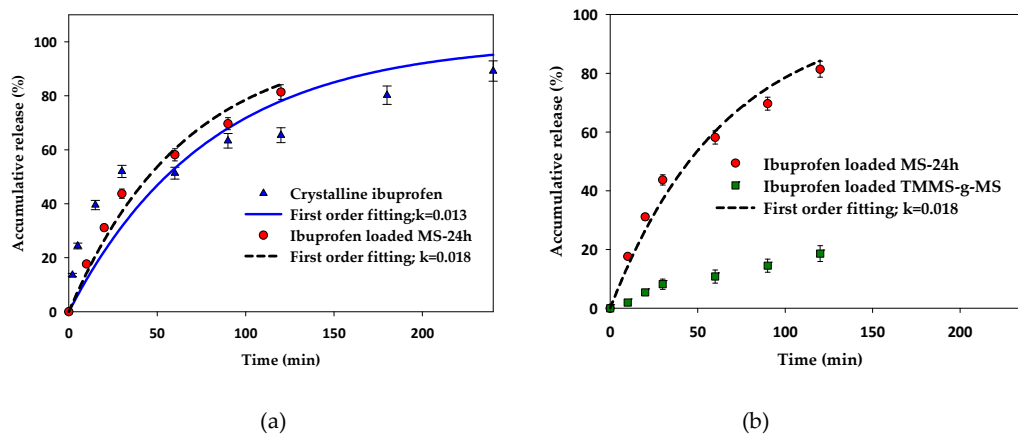
224

225

226

227

In vitro release tests were carried out for ibuprofen-loaded mesoporous silica and surface modified mesoporous silica aerogels and compared with the crystalline ibuprofen. The dissolution tests were conducted under the sink condition for all experiments to avoid the solubility effect. As illustrated in Figure 9, the release rate of crystalline ibuprofen was similar to the release of ibuprofen-loaded MS-24h in the first 60 min and became slower after that whereas the release rate of ibuprofen-loaded MS-24h was faster after 60 min. The first order kinetics fit well with the release of ibuprofen-loaded MS-24h. In the case of ibuprofen-loaded TMMS-g-MS (Figure 9(b)), the release rate was much slower than that of crystalline ibuprofen and ibuprofen-loaded MS-24h.



228

229

230

231

232

Figure 9. Accumulative release of (a) crystalline ibuprofen compared with ibuprofen-loaded MS-24h and (b) ibuprofen-loaded MS-24h compared with ibuprofen-loaded TMMS-g-MS with first order kinetics model fitting

233

4. Discussion

234

235

236

237

238

239

240

The work started with the green synthesis of mesoporous silica using glycerol. The reaction was carried out with two different sources of silica, namely rice husk ash and fumed silicas. The latter source of silica was very pure, whereas the former one had some trace impurities. The dependency of hydrolysis-ageing time on the physico-chemical properties of as-synthesized mesoporous silicas revealed that the longer the ageing time, the larger the BET surface area. It was found from Table 1 that after reaction and calcination, the silica composition of MS-24h increased from 87 to 95 %wt. All prepared mesoporous silicas were amorphous as analyzed by XRD (data not shown). Silica contents

241 were increased upto 95 %wt and unaffected by hydrolysis-ageing periods. These organic residues (4-
242 6 %wt) could result from the remaining organic compounds in porous silica structures or incomplete
243 elimination after calcinations [12]. The results showed that the hydrolysis-ageing time influenced the
244 BET surface area, pore volume and pore size. At 120 h of hydrolysis-ageing time, BET surface area
245 reached 500.7 m²/g and the pore volume and pore diameter were 0.655 cm³/g and 5.23 nm respectively.
246 FTIR confirmed the reduction of silanol peak intensities, or more condensation could occur. The
247 surface modification of MS-24h with TMMS showed the hydrophobic nature, but preserved BET
248 surface area, pore volume and pore diameter.

249 According to our previous study [13], ibuprofen was highly soluble in supercritical carbon
250 dioxide, the high adsorption on porous aerogels was achieved. Such extraordinarily high loadings
251 could indicate that multilayer adsorption or even capillary condensation took place. From Figure
252 7(b), the drug loading of MS-24h was 6 times higher than TMMS-g-MS. Ibuprofen has one aromatic
253 ring and a relatively long and flexible hydrophobic moiety (butyl group). As a result of that, the
254 ibuprofen molecules could favourably pack on the surface, leading to a high adsorption [13].
255 However, after the surface modification of MS-24h with TMMS, some surface hydroxyl groups were
256 randomly substituted by trimethyl groups. The heterogeneous surface chemistry might be
257 responsible for poor adsorption.

258 Although the ibuprofen adsorbed on the MS could be in an amorphous state, the release was not
259 significantly enhanced. Smirnova I. and colleagues [18, 19] reported that the loading of drug onto
260 very large surface area of silica aerogels using supercritical carbon dioxide was advantageous in
261 terms of the change of crystalline to amorphous drugs, which was consequently responsible for the
262 faster dissolution and hence release rate. In this case, the effect of dissolution of amorphous ibuprofen
263 was less pronounced. This may be due to the low solubility of ibuprofen in the test media (0.1 M
264 HCl). The release profile of ibuprofen-loaded MS-24h was fitted well with the first order release
265 kinetics shown in equation (1).

$$266 \quad \ln C_t = \ln C_0 + K_1 t \quad (1)$$

267 where C_t is the amount of drug dissolved at interval time t , C_0 is the initial amount of the drug in the
268 solution, and k_1 is the first order constant.

269 In the case of the release kinetics of ibuprofen-loaded TMMS-g-MS, much slower release
270 kinetics of ibuprofen-loaded TMMS-g-MS is observed. This might be due to more hydrophobic
271 nature of this material. Hydrophobic mesoporous silica is more stable in a dissolution medium (e.g.
272 0.1 M HCl) and pharmaceuticals release would be controlled by the molecular diffusion of the drug
273 from the adsorption site (on the surface or in pores) and the penetration of dissolution medium
274 through the porous structure [13]. Thus, the slower release can be expected.

275 5. Conclusions

276 Mesoporous silica materials at various hydrolysis-ageing periods were prepared from rice husk
277 ash starting materials. High surface area mesoporous silica was obtained at optimal hydrolysis-
278 ageing period of 120 h (500.7 m²/g BET surface area, 0.655 cm³/g pore volume and 5.23 nm pore
279 diameter). The increase in hydrolysis-ageing periods decreases the size of pores. N₂ sorption
280 isotherms and TEM images revealed the changes in hysteresis and pore structures. Prepared
281 mesoporous silica was successfully modified by trimethoxymethylsilane. The methyl moiety was
282 responsible for the hydrophobic characteristic. This method provides a sustained route for renewable
283 materials and can potentially be used for various applications. The adsorption of ibuprofen on the
284 mesoporous silicas; MS-24h and TMMS-g-MS, depended on the chemical structure. % loading of
285 Ibuprofen-loaded MS-24h was 6 times higher than that of Ibuprofen-loaded TMMS-g-MS. The release
286 kinetics of Ibuprofen-loaded TMMS-g-MS was much slower than that of crystalline and Ibuprofen-
287 loaded MS-24h. This was due to the diffusion control of the dissolution medium. The hydrophobic
288 characteristic was more stable in the medium, while in the case of Ibuprofen-loaded MS-24h, the

289 release profile was closed to the crystalline ibuprofen. The slow release rate of ibuprofen-loaded MS
290 will allow for the controlled release kinetics.

291 **Acknowledgments:** The study was supported by Thailand Research Fund and Office of the. Higher Education
292 Commission grant no. MRG5180152. The authors acknowledge the Department of Materials Science and
293 Engineering, Faculty of Engineering and Industrial Technology, Silpakorn University. Evonik Thailand is
294 acknowledged for materials supply.

295 References

- 296 1. GIEWS *Crop prospects and food situation*. 2017.
- 297 2. Yalçın, N.; Sevinç, V. Studies on silica obtained from rice husk. *Ceram Int* **2001**, *27*, pp. 219-224,
298 10.1016/S0272-8842(00)00068-7.
- 299 3. Della, V.P.; Kuhn, I. Rice husk ash as an alternate source for active silica production. *Mater Lett* **2002**,
300 *57*, pp. 818-821, [http://www.sciencedirect.com/science/article/B6TX9-4625R5D-](http://www.sciencedirect.com/science/article/B6TX9-4625R5D-1/2/422c3984b452c26411de9fe30479494a)
301 [1/2/422c3984b452c26411de9fe30479494a](http://www.sciencedirect.com/science/article/B6TX9-4625R5D-1/2/422c3984b452c26411de9fe30479494a)
- 302 4. Chareonpanich, M.; Namto, T. Synthesis of ZSM-5 zeolite from lignite fly ash and rice husk ash. *Fuel*
303 *Process Technol* **2004**, *85*, pp. 1623-1634, [http://www.sciencedirect.com/science/article/B6TGF-3VN3V0P-](http://www.sciencedirect.com/science/article/B6TGF-3VN3V0P-D/2/bd5910ba87030d99452bc2826c86dd32)
304 [4D034MD-2/2/144a507319af441399735aac7ab220c7](http://www.sciencedirect.com/science/article/B6TGF-3VN3V0P-D/2/bd5910ba87030d99452bc2826c86dd32)
- 305 5. Prasetyoko, D.; Ramli, Z. Conversion of rice husk ash to zeolite beta. *Waste Management* **2006**, *26*, pp.
306 1173-1179, [http://www.sciencedirect.com/science/article/B6VFR-4HH81D8-](http://www.sciencedirect.com/science/article/B6VFR-4HH81D8-2/2/3c592bae718e5d8c3613ebcad0a1b26b)
307 [2/2/3c592bae718e5d8c3613ebcad0a1b26b](http://www.sciencedirect.com/science/article/B6VFR-4HH81D8-2/2/3c592bae718e5d8c3613ebcad0a1b26b)
- 308 6. Wang, H.P.; Lin, K.S. Synthesis of zeolite ZSM-48 from rice husk ash. *J Hazard Mater* **1998**, *58*, pp. 147-
309 152, [http://www.sciencedirect.com/science/article/B6TGF-3VN3V0P-](http://www.sciencedirect.com/science/article/B6TGF-3VN3V0P-D/2/bd5910ba87030d99452bc2826c86dd32)
310 [D/2/bd5910ba87030d99452bc2826c86dd32](http://www.sciencedirect.com/science/article/B6TGF-3VN3V0P-D/2/bd5910ba87030d99452bc2826c86dd32)
- 311 7. Li, X.; Shi, J. A template route to the preparation of mesoporous amorphous calcium silicate with high
312 in vitro bone-forming bioactivity. *J Biomed Mater Res B Appl Biomater* **2007**, *83B*, pp. 431-439,
313 [http://www.ncbi.nlm.nih.gov/entrez/query.fcgi?cmd=Retrieve&db=PubMed&dopt=Citation&list_uids](http://www.ncbi.nlm.nih.gov/entrez/query.fcgi?cmd=Retrieve&db=PubMed&dopt=Citation&list_uids=17415771)
314 [=17415771](http://www.ncbi.nlm.nih.gov/entrez/query.fcgi?cmd=Retrieve&db=PubMed&dopt=Citation&list_uids=17415771)
- 315 8. Vempati, R.K.; Borade, R. Template free ZSM-5 from siliceous rice hull ash with varying C contents.
316 *Microporous and Mesoporous Mater* **2006**, *93*, pp. 134-140, <Go to ISI>://000239252700016
- 317 9. Wittoon, T.; Chareonpanich, M. Synthesis of bimodal porous silica from rice husk ash via sol-gel
318 process using chitosan as template. *Mater Lett* **2008**, *62*, pp. 1476-1479,
319 [http://www.sciencedirect.com/science/article/B6TX9-4PMB3Y1-](http://www.sciencedirect.com/science/article/B6TX9-4PMB3Y1-3/2/8c663a67efe4e388f616eb9b3db02fac)
320 [3/2/8c663a67efe4e388f616eb9b3db02fac](http://www.sciencedirect.com/science/article/B6TX9-4PMB3Y1-3/2/8c663a67efe4e388f616eb9b3db02fac)
- 321 10. Sa'nchez-Flores, N.A.; Pacheco-Malago'n, G. Mesoporous silica from rice hull ash. *J Chem Technol*
322 *Biotechnol* **2007**, *82*, pp. 614-619,
- 323 11. Pacheco G; P'erez P. Local order in depolymerized silicate lattices. *Inorg Chem* **2005**, pp. 8486-8494,
- 324 12. Suttiruengwong, S.; Puathawee, P. Preparation of Mesoporous Silica from Rice Husk Ash: Effect of
325 Depolymerizing Agents on Physico-Chemical Properties. *Adv Mat Res* **2010**, *93-94*, pp. 664-667,
326 10.4028/www.scientific.net/AMR.93-94.664.
- 327 13. Suttiruengwong, S. Silica Aerogels and Hyperbranched Polymers as Drug Delivery Systems. Doctor
328 of Engineering Degree, Fridrich Alexander Univeristy Erlangen Nuremberg, 3 August 2005.
- 329 14. NIST. *Thermophysical Properties of Fluid Systems*. 2018 [cited 2016 23 May 2017]; Available from:
330 <https://webbook.nist.gov/chemistry/fluid/>.

- 331 15. Liou, T.H. Preparation and characterization of nano-structured silica from rice husk. *Materials Science*
332 *and Engineering a-Structural Materials Properties Microstructure and Processing* **2004**, *364*, pp. 313-323,
333 10.1016/j.msea.2003.08.045.
- 334 16. Zong, S.; Wei, W. Characterization and comparison of uniform hydrophilic/hydrophobic transparent
335 silica aerogel beads: skeleton strength and surface modification. *RSC Advances* **2015**, *5*, pp. 55579-
336 55587, 10.1039/C5RA08714G.
- 337 17. Rouquerol, F.; Rouquerol, J. *Adsorption by powders and porous solids*; Academic Press: New
338 YorkAcademic Press, 1999; pp. 303-320,
- 339 18. Smirnova, I.; Suttiruengwong, S. Dissolution rate enhancement by adsorption of poorly soluble drugs
340 on hydrophilic silica aerogels. *Pharm Dev Technol* **2004**, *9*, pp. 443-52, 10.1081/PDT-200035804.
- 341 19. Smirnova, I.; Suttiruengwong, S. Feasibility study of hydrophilic and hydrophobic silica aerogels as
342 drug delivery systems *J. Non-Cryst. Solids* **2004**, *350*, pp. 54-60,
343 [http://www.ncbi.nlm.nih.gov/entrez/query.fcgi?cmd=Retrieve&db=PubMed&dopt=Citation&list_uids=](http://www.ncbi.nlm.nih.gov/entrez/query.fcgi?cmd=Retrieve&db=PubMed&dopt=Citation&list_uids=15581080)
344 [15581080](http://www.ncbi.nlm.nih.gov/entrez/query.fcgi?cmd=Retrieve&db=PubMed&dopt=Citation&list_uids=15581080)
- 345
346
347
348
349
350